A Study of SiC/Ni Composite Plating in the Watts Bath

By S.H. Yeh & C.C. Wan

Codeposition behavior of SiC powders with Ni under various conditions was studied. In the low-current-density region, codeposition follows the two successive adsorption steps first proposed by Guglielmi. On the other hand, codeposition is a function of powder transfer control in the high-current-density region. These predictions were verified experimentally. In addition, the effect of stir on the volume fraction of SiC powders in the deposit was also investigated.

Composite coatings[1-7] were obtained by plating in an electrolyte having suspended inert powders, such as oxides, carbides, borides, or nitrides, etc. These coatings usually show good corrosion, oxidation and wear resistance, and they have been widely used in self-lubricating[8] and dispersion-hardening applications.[9,10] Because the quantity and distribution of powders in a deposit determine the physical properties of a composite coating, it is necessary to understand the mechanisms of codeposition in order to control the process more effectively.

A well-known adsorption model was postulated by Guglielmi,[11] in which a two-step successive adsorption was proposed as follows:

$$\frac{C}{\alpha} = \frac{Mi_0}{nFdV_0} e^{(A_0-B_0)\eta} \left[\frac{1}{K} + C\right] \qquad (1)$$

where C is the volume fraction of powders in the electrolyte, η is the volume fraction of powders in the deposit, n is the valence of the electrodeposited metal, M is its atomic weight, d is its density, A_o, B_o, V_o and K are constants, i_o is the exchange current density, and η is the cathodic overpotential. Guglielmi studied TiO_2/Ni and SiC/Ni systems and found that there was a linear relationship between C/α and C, which was derived from Eq. (1). According to Guglielmi's model, the powders were first loosely adsorbed on the surface of the cathode, then entrapped in the deposit as a result of strong adsorption behavior by the subsequently applied electrical field. This model was later verified by Celis and Roos,[12] using an Al_2O_3/Cu system, by Masuko and Mushiake[13] using an Al_2O_3/Ni system, and by Totlani and Athavale,[14] using a TiO_2/Cu system.

In addition, Celis, Roos and Buelens[15] also derived a model based on a statistical approach to the incorporation behavior of powders. A basic hypothesis of this model was that an adsorbed layer of ionic species was formed around the surface of the inert powders. The adsorbed ions were reduced to metal as part of the matrix for the incorporation of powders during reduction. This model could be translated into the following expression,

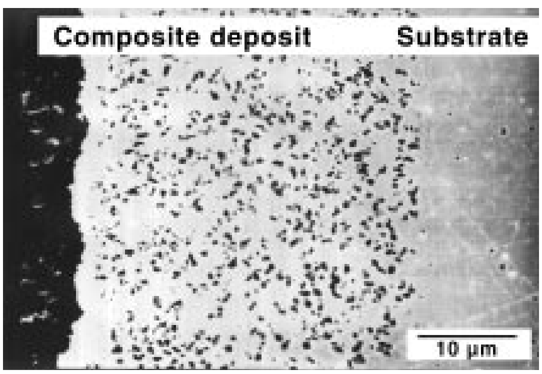

Fig. 1—SEM photograph of cross section of composite layer of SiC/Ni produced in Watts bath with 0.63% SiC; 18 mA/cm².

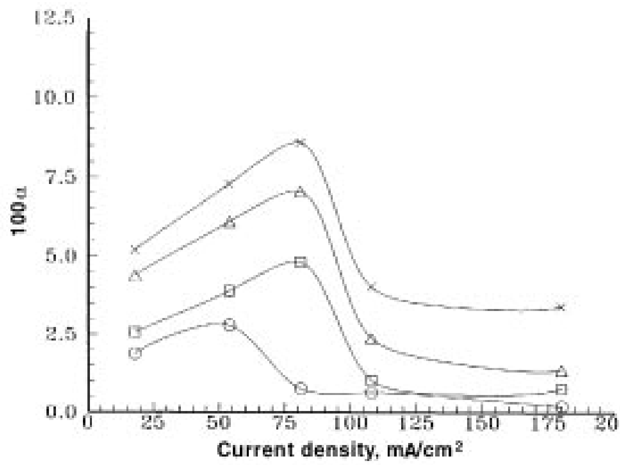

Fig. 2—Effect of current density on volume fraction of SiC powder in deposit with different powder contents at stir rate 100 rpm: (❍) 0.32% (v/o); (❑) 0.63% (v/o); (△) 1.25% (v/o); (X) 2.48% (v/o).

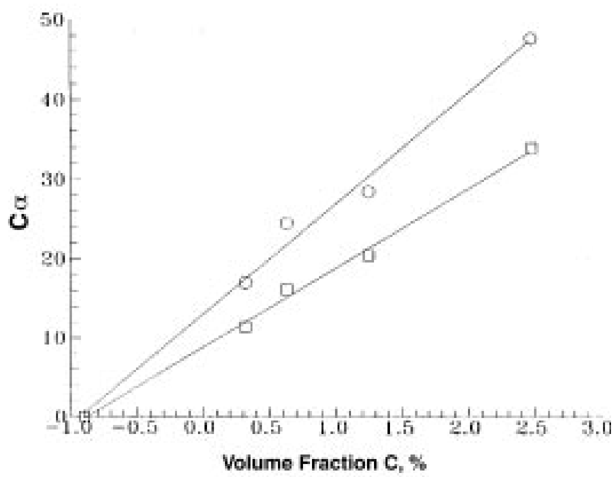

Fig. 3—Relationship between C/α and C, according to Eq. (1) at low current density: (❍) 18 mA/cm²; (❑) 54 mA/cm².

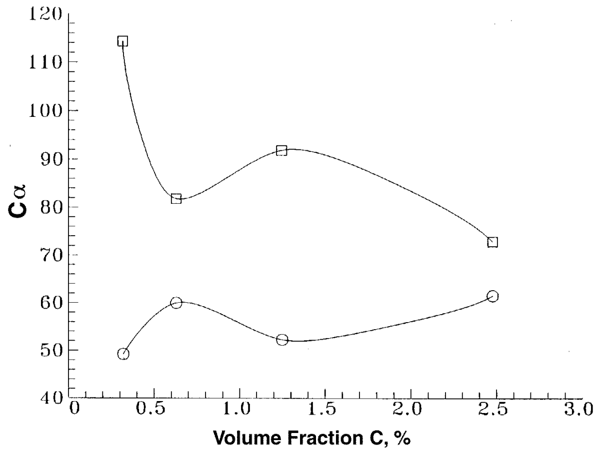

Fig. 4—Relationship between C/α and C, according to Eq. (1) at high current density: (❍) 108 mA/cm²; (❑) 180 mA/cm².

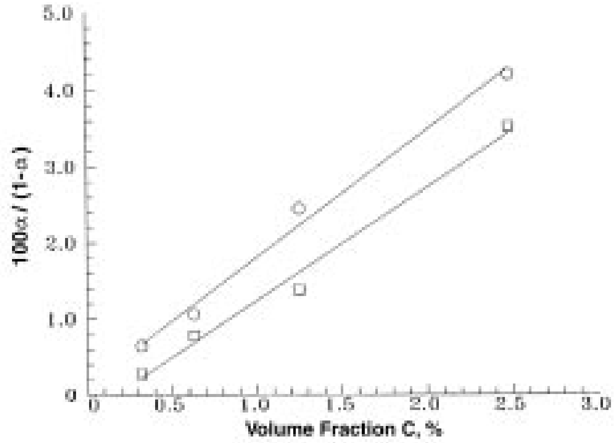

Fig. 5—Relationship between α/(1 - α) and C, according to Eq. (8) at stir rate of 100 rpm. (❍) 108 mA/cm²; (❑) 180 mA/cm².

$$\text{w/o powder embedded} = \frac{W_p N_p P}{\Delta W + W_p N_p P} 100 \qquad (2)$$

where W_p is the weight of powder (kg), N_p is the amount of powder crossing the diffusion layer at the working electrode per unit time and surface area ($sec^{-1}m^{-2}$), P is the probability of the incorporation of powder at current density I, ΔW_m is the mass of metal matrix deposited per unit time and surface area ($kg^{-2}sec^{-1}$).

Suzuki and Asai[16,17] studied the deposition mechanism of Al_2O_3/Ag from silver thiocyanate solution for different particle sizes, fluid velocities, and cathodic overvoltages. They found that Al_2O_3 particles in the deposit would suppress the electrodeposition of silver, but that thorough stir near the electrode surface promoted deposition. In addition, the adsorption energy of Al_2O_3 on the electrode surface was also calculated.

Although the two-step adsorption model has been verified by many researchers,[13-15] the model does not take into account the effect of hydrodynamic conditions. Eq. (2) does include the effect of convection, but it is quite difficult to measure or calculate these parameters. The main objective of this research, therefore, was to propose a new mechanism for the SiC/Ni system, which can include the effect of powder transfer by fluid flow.

Experimental Procedure

The composite coatings of nickel with SiC powders were obtained from the Watts bath. The basic compositions of electrolyte and plating conditions were:

$NiSO_4 \cdot 6H_2O$	350 g/L
$NiCl_2 \cdot 6H_2O$	45 g/L
H_3BO_3	35 g/L
α-SiC powders	10 g/L ~ 80 g/L
pH	4.0 ±0.2
Temperature	50 ±1 °C
Current density	18 mA/cm² ~ 180 mA/cm²
Stir rate	75 rpm ~ 300 rpm

All chemicals used were EP grade. The SiC powders have an average particle size of about 1.5 µm in diameter and density about 3.21.

The electrolyte with SiC powders was stored in a 500-mL beaker and was stirred for at least one day prior to plating. An optical microscope was employed to check the dispersion of the suspension. The cathode was Ni foil of 99.9 percent purity and was masked on one side. The anode was a pure Ni plate. The quantities of SiC in the deposit were determined by the gravimetric method. The composite coatings were first dissolved in 50-percent nitric acid, then the solution was filtered. The SiC powders left behind were weighed after firing at 600 °C.

Results and Discussion

Figure 1 shows a typical cross section of SiC/Ni composite coating examined by SEM. In the photograph, the small dark dots with different shapes and sizes in the deposit are SiC powder. It is clear that the distribution of SiC powder is quite even. To count the volume fraction of SiC powder in the deposit, nitric acid was used to dissolve the deposit, and the residual SiC powder was separated.

Effect of Plating Current Density

Figure 2 shows the relationship between the volume fraction of SiC powder in the deposit (α) and the current density for different powder content in the electrolyte (C). It seems that α increases with increasing C at the same current density. In addition, α increases initially with the current density, I, and reaches a maximum at I_{max}, then decreases. A similar result was also found by White and Forster[18] with an Al_2O_3/Cu system. It is apparent from Fig. 2 that the maximum appears at I_{max} = 81 mA/cm² in all cases except when the volume fraction "C" is 0.32 percent (v/o). In that case, I_{max} is 54 mA/cm². The codeposition behavior of SiC/Ni, therefore, can be divided into two regions—one when the current density is less than I_{max} (low-current-density region). The other region is for current density larger than I_{max} (high-current-density region).

Codeposition of SiC/Ni at current density less than I_{max} was different from that at current density greater than I_{max}.

Accordingly, Fig. 2 was reorganized into Figs. 3 and 4 by choosing I_{max} as a dividing current density. When the current density is less than I_{max}, the relationship between C/α and C is a linear, as shown in Fig. 3. When the current density is greater than I_{max}, C/α vs. C is no longer a linear, as shown in Fig.4. Therefore, if the current density is less than I_{max}, the codeposition behavior of SiC/Ni matches Guglielmi's two-step adsorption model (*i.e.*, powders are adsorbed loosely on the electrode surface initially, then the loose adsorption

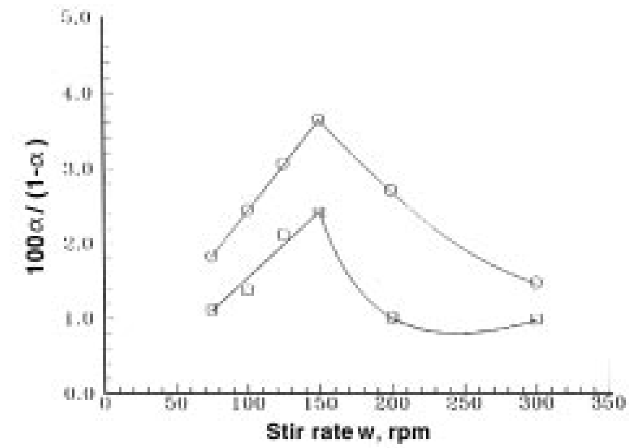

Fig. 6—Relationship between α/(1 - α) and w, according to Eq. (9), with 1.25% SiC powder: (❍) 108 mA/cm²; (❑) 180 mA/cm².

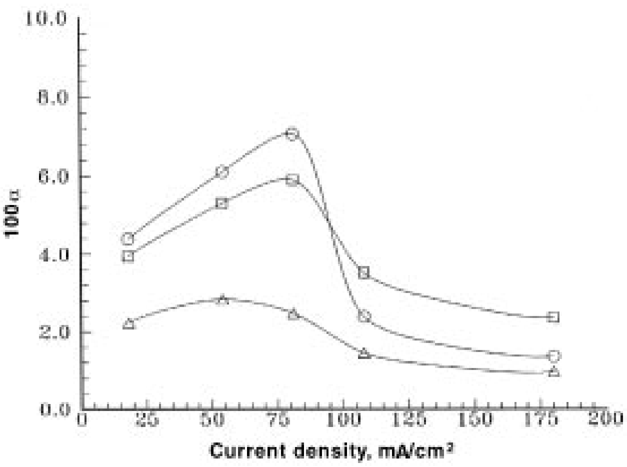

Fig. 7—Effect of current density on the volume fraction of SiC powder in deposit for different stir rates: (❍) 100 rpm; (❑) 150 rpm; (△) 300 rpm.

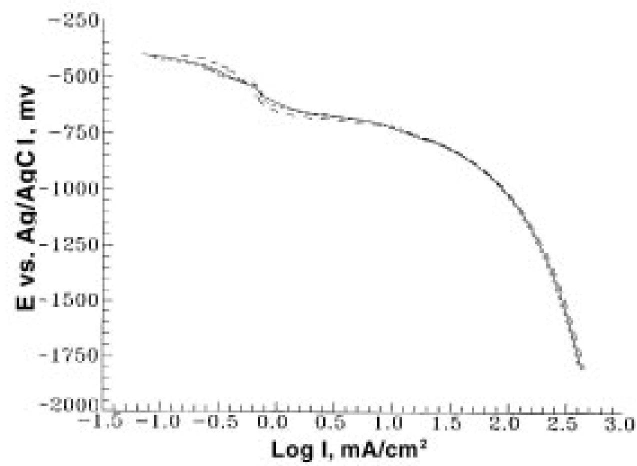

Fig. 8—Polarization curves of the Watts bath with different SiC powder content: (—) no SiC; (- - -) with 0.63% (v/o); (- - - -) with 1.25% (v/o).

progresses to strong adsorption under the influence of the applied electric field). Moreover, the higher α appeared at the lower plating current density, 18 mA/cm², shown in Fig. 3. This is also consistent with Guglielmi's findings.

When the current density is greater than I_{max}, the codeposition of SiC/Ni does not follow Guglielmi's model. This is because the SiC powder does not have enough time to be adsorbed loosely on the surface of the electrode at high current density. Codeposition of SiC/Ni in this case cannot be adequately described by an adsorption control model. It is necessary, therefore, to derive a new model for the codeposition of SiC/Ni in the high-current-density region.

First, a relationship between the stir rate and the transfer rate of the electrolyte can be represented as follows,

$$v = fw \qquad (3)$$

where v is the transfer rate of the electrolyte (cm/sec), f is a transfer factor to convert the magnetic stir rate into the transfer rate of the electrolyte, and w is the stir rate of the magnetic stirrer (rpm). The volume of powder transferred to the electrode per unit time may be expressed as follows,

$$\text{Volume of powder near the electrode} = vAC = fwAC \qquad (4)$$

where A is the apparent area of the electrode.

The concentration of SiC powder in the deposit can now be expressed as

$$\alpha = \frac{V_p}{V_{Ni} + V_p} \qquad (5)$$

where V_{Ni} is the volume occupied by Ni in the deposit, and V_p is the volume occupied by SiC powders in the deposit.

The volume of Ni deposited per second can be deduced from Faraday's Law,

$$V_{Ni} = \frac{\xi IMA}{nFd} \qquad (6)$$

where ξ is the current efficiency and I is the current density.

By substituting Eq. (6) into Eq. (5), and we obtain

$$V_p = V_{Ni}\frac{\alpha}{1-\alpha} = \frac{\xi IMA}{nFd}\,\frac{\alpha}{1-\alpha} \qquad (7)$$

Assuming that the powder transferred to the electrode is totally incorporated into the Ni matrix, we can make a transient mass balance for the powder during electrodeposition. In this case, Eq. (4) should be equal to Eq. (7), which can be rearranged in the following form:

$$\frac{\alpha}{1-\alpha} = \frac{nFdfw}{\xi IM}C \qquad (8)$$

Physically, this means that the ratio of V_p/V_{Ni} is proportional to the powder concentration in the electrolyte at a constant current density and magnetic stir rate.

Figure 5 is the reorganized result of Fig. 2 at 108 mA/cm² and 180 mA/cm², which confirms the validity of Eq. (8). The relationship between 100 α/(1 - α) and C is linear. In addition, at lower current density, 108 mA/cm², the system has a greater slope (about 1.67) than the other system (about 1.38) at higher current density, 180 mA/cm². The difference of slope mainly results from difference of ξI, as shown by Eq. (8).

Consequently, Eq. (8) could describe the system very well in the high-current-density region, and the codeposition behavior of SiC/Ni is controlled by the transfer rate of the powder in this case. The growth of the nickel coating is very quick, so that the powder would be entrapped in the growing deposit quickly; there is not enough contact time for the transferred powder to be adsorbed loosely on the electrode surface.

Effect of Stir Rate

To check the codeposition of SiC/Ni again in the high-current-density region under different stir rates, Eq. (8) can be rearranged:

$$\frac{\alpha}{1-\alpha} = \frac{nFdfC}{\xi IM} w \qquad (9)$$

The relationship between 100 $\alpha/(1-\alpha)$ and w is shown in Fig. 6. The quantity $\alpha/(1-\alpha)$ increases linearly with stir rate w until the rate reaches 150 rpm, then decreases with the stir rate. The codeposition behavior of SiC/Ni is apparently controlled by powder transfer when the stir rate is smaller than 150 rpm. The reason that $\alpha/(1-\alpha)$ decreases with very rapid stir is a result of the collision factor. When the quantity of the transferred powder is too great to be completely entrapped by the growing matrix, the free powder particles from the electrode collide with the oncoming particles. This collision factor results, therefore, in the decrease of α, as well as of $\alpha/(1-\alpha)$. In fact, Lee[19] also found that content of alumina powder in a Cu deposit reached a maximum as the flow rate was increased to 5 cm/sec, then decreased if the flow rate was further increased.

Previously, the effect of rotation speed on the quantity of powder in the deposit was discussed, using a rotating disk[17,20] or electrode.[21] They found that the powder in the deposit decreased with increasing rotation speed, but did not find a maximum with respect to rotation speed. The seeming difference from our results could be attributed to: (1) the rotating electrode would increase the collision frequency of powder particles with the electrode, which decreases the deposition of powder in the deposit as the rotation speed is increased; (2) if the codeposition of powder is a function of adsorption control at the applied current density. The freshly transferred powder could not be effectively adsorbed on the electrode when the rotation speed was too high.

Figure 7 shows that 100 α also exhibits a maximum value with respect to the current density, I. Codeposition of SiC/Ni should be under adsorption control before 100 α reaches the maximum value and, in this case, the SiC powder is adsorbed loosely on the electrode. Its quantity should decrease because of increased transfer by the electrolyte. This accounts for the decrease of α as the stir rate increases from 100 to 300 rpm.

When the current density is greater than I_{max}, however, the system becomes powder-transfer-controlled. A higher stir rate could increase the powder transfer rate, but at very high stir rates (*e.g.*, 300 rpm), excessively rapid powder transfer adversely affects deposit composition because of the collision factor, as previously discussed.

Current Efficiency with Different SiC Contents At High Current Density

Vol. Fraction %	Efficiency %	
	108 mA/cm^2	180 mA/cm^2
0	94.4	92.0
0.32	93.5	91.5
0.63	92.6	92.5
1.25	94.2	91.0

Effect of Current Efficiency

The polarization behavior of the Ni/SiC system was measured and is shown in Fig. 8, which represents two consecutive reduction reactions: H^+ and Ni^{+2}, reduced to H_2 and Ni. This phenomenon was also noticed by Hoare;[22] he further found that the reduction of H^+ would occur more quickly than the reduction of Ni^{+2} with an increasing reduction potential. Generally, both reactions would occur in a Watts bath, and hydrogen evolution results in decrease of current efficiency. Figure 8 also shows that there is little difference as SiC powder was added in the Watts bath. This means that the powder would not significantly affect the electrochemical reaction of nickel ions.

The table reports the effect of SiC powder on current efficiency, which seems weakly influenced by the powder, consistent with the results shown in Fig. 8. Therefore, the value of ξI in Eq. (8) can be taken as a constant at a given plating current density and the equation could satisfactorily describe the codeposition behavior of SiC/Ni in the high-current-density region.

Symbols

A	Apparent area of electrode
A_0	Constant
α	Volume fraction of powders in the deposit
B_0	Constant
C	Volume fraction of powders in the electrolyte
d	Density of the deposition metal
f	A transfer factor to convert the magnetic stir rate into the transfer rate of the electrolyte
I	Applied current density
i_0	Exchange current density
K	Constant
M	Atomic weight of the deposited metal
N_p	Amount of powder crossing the diffusion layer at the working electrode per unit time and surface ($sec^{-1}m^{-2}$)
n	Valence of the electrodeposited metal
P	Probability of the incorporation of powder at current density I
V_0	Constant
V_{Ni}	Volume occupied by Ni in the deposit
V_p	Volume occupied by SiC powders in the deposit
v	Transfer rate of the electrolyte (cms^{-1})
W_p	Weight of powder (kg)
W_m	Mass of metal matrix deposited per unit time and surface area ($kg^{-2}sec^{-1}$)
w	Stir rate of magnetic stirrer
η	Cathodic overpotential
ξ	Current efficiency

Summary

In the low-current-density region, codeposition of SiC with Ni in a Watts bath falls within adsorption control, and it matches the Guglielmi two-step adsorption model. Higher powder content in the electrolyte increases adsorption, resulting in a higher volume fraction of powder in the deposit after plating. Moreover, high stir rate and high powder transfer rate adversely affect the adsorbed powder and decrease its volume fraction in the deposit.

At high current density, there is not enough time for the transferred SiC powder to be adsorbed on the electrode during plating. The codeposition behavior becomes powder-transfer-controlled. The volume fraction of powder increases as the powder transfer rate increases, but a high stir rate tends to decrease the volume fraction of powder, because of the collision factor.

Editor's note: *Manuscript received, December 1993; revision received, December 1996.*

References

1. J. Zahavi and H. Kerbel, *Plat. and Surf. Fin.*, **69**, 76 (Jan. 1982).
2. J. Foster and E. Cameron, *Trans. Inst. Met. Fin.*, **54**, 178 (1976).
3. E.C. Kedward, C.A. Addison and A.A. Tennett, *Trans. Inst. Met. Fin.*, **54**, 8 (Jan. 1976).
4. M. Pushpavanam and B.A. Shenoi, *Metal Fin.*, **75**, 38 (Apr. 1977).
5. V.P. Greco, *Plat. and Surf. Fin.*, **7**, 62 (1989).
6. J. Sadowska-Mazur, M.E. Warwick and R. Walker, *Trans. Inst. Met. Fin.*, **64**, 142 (1986).
7. R. Narayan and S. Chattopathyay, *Surf. Tech.*, **16**(3), 227 (1982).
8. J.M. Sykes and D.J. Alner, *Trans. Inst. Met. Fin.*, **56**, 92 (1978).
9. E. Anderson, *J. Mater. Sci.*, **8**, 676 (1973).
10. P.J.E. Forsyth, R.W. George and D.A. Ryder, *Appl. Mater. Res.*, **3**, 223 (1964).
11. N. Guglielmi, J. *Electrochem. Soc.*, **119**, 1009 (1972).
12. J.P. Celis and J.R. Roos, *J. Electrochem. Soc.*, **124**, 1508 (1977).
13. N. Masuko and K. Mushiake, *J. Electrochem. Soc.* (India), **31**, 119 (1982).
14. M.K. Tolani and S.N. Athavale, *J. Electrochem. Soc.*, **134**, 102 (1987).
15. J.P. Celis, J.R. Roos and C. Buelens, J. *Electrochem. Soc.*, **134**, 1402 (1987).
16. Y. Suzuki, M. Wajima and O. Asai, *J. Electrochem. Soc.*, **133**, 259 (1986).
17. Y. Suzuki and O. Asai, *J. Electrochem. Soc.*, **134**, 1905 (1987).
18. C. White and J. Foster, *Trans. Inst. Met. Fin.*, **59**, 8 (1981).
19. C.C. Lee and C.C. Wan, *J. Electrochem. Soc.*, **135**, 1930 (1988).
20. C. Buelens, J.P. Celis, and J.R. Roos, *J. Appl. Electrochem.*, **13**, 541 (1983).
21. R. Bazzard and P.J. Boden, *Trans. Inst. Met. Finish.*, **50**, 63 (1972).
22. J. P. Hoare, *J. Electrochem. Soc.*, **133**, 2491 (1986).

About the Authors

Shinn-Horng Yeh is a research scientist, Surface and Coating Technology Laboratory, Materials Research Laboratories, Industrial Technology Research Institute, 195 Chung Hsing Rd., Section 4, Bldg 77, Chutung, Hsinchu, Taiwan 31015, Republic of China. He is a PhD candidate in chemical engineering, National Tsing Hua University, Taiwan. He holds an MS in chemical engineering from the National Tsing Hua University and a BS in chemical engineering from the Chung Yuan Christian University.

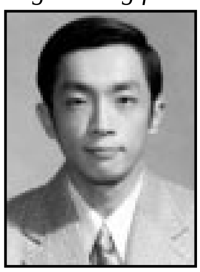

Chi-Chao Wan is professor of chemical engineering at the National Tsing Hua University, Hsinchu, Taiwan. Dr. Wan is a past president of the AESF Taipei Branch, and his major research interest is in surface treatments for the printed circuit board industry, as well as plating, electrochemistry and metal finishing.